Colloid Polym Sci 277:1172–1178 (1999)
© Springer-Verlag 1999

ORIGINAL CONTRIBUTION

M. Siddiq
K.C. Tam
R.D. Jenkins

Dissolution behaviour of model alkali-soluble emulsion polymers: effects of molecular weights and ionic strength

Received: 15 February 1999
Accepted in revised form: 13 July 1999

M. Siddiq · K.C. Tam (✉)
School of Mechanical and Production Engineering
Nanyang Technological University
Nanyang Avenue, Singapore 639798
Singapore

R.D. Jenkins
Union Carbide Asia Pacific Inc.
Technical Center, 16 Science Park Drive
The Pasteur, Singapore 118227, Singapore

Abstract The dissolution behaviour of model alkali-soluble polymer emulsions with different molecular weights was studied using conductometric and potentiometric titration and laser light scattering techniques. The behaviour of the copolymer was studied as a function of the degree of neutralisation, α = [NaOH]/[COOH]. The polymer latex swells with increasing α values up to $\alpha = 0.5$–0.7, after which the dissociation of polymer chains commences. At $\alpha = 1.0$, all the polymer latexes dissociate into individual polymer chains. By combining the results of static and dynamic laser light scattering, we observed that the polymers have a compact conformation at $\alpha = 0$. This compact conformation changes to a random coil at around $\alpha = 0.5$, which then becomes a fully extended coiled conformation at $\alpha = 1.0$, when all the COOH polymer groups are hydrolysed. The dissolution of low-molecular-weight polymers is faster than that of high-molecular-weight polymers.

Key words Dissolution · Molecular weights · Ionic strength · Neutralisation · Light scattering

Introduction

Hydrophobically modified water-soluble polymers have attracted much interest in recent years [1–14]. These polymers are widely used in industries for paint formulation and paper coating. Such polymers are commonly referred to as associative thickeners. The three most important types of commercial associative polymers are

1. Hydrophobically modified ethylene oxide urethane (HEUR) block copolymer.
2. Hydrophobically modified hydroxyethyl cellulose (HMHEC).
3. Hydrophobically modified alkali-soluble emulsion (HASE) polymer.

Hydrophobically modified water-soluble polymers undergo self-association in aqueous solution by virtue of their hydrophobic groups. The association can be either intramolecular or intermolecular or both, depending on the microstructure of the polymer and the size of the hydrophobes. At low concentration, these associative polymers form a micellelike structure, and the size gradually increase with the increasing polymer concentration. The solution properties of these polymers have been studied using a wide range of techniques, including viscosity [15–18], static and dynamic fluorescence [19, 20], static and dynamic laser light scattering (LLS) and microcalorimetry [21, 22].

While much research has largely been focused on the HEUR and HMHEC [5, 23–27] systems, relatively few studies have been carried out with HASE polymers. HASE polymers can be classified as hydrophobically modified anionic polyelectrolytes. They are manufactured as low-pH latexes, and contain acid groups along the polymer backbone. When neutralised in aqueous solution with a suitable base, the latex particles are ionised as a result of an acid–base reaction. The partially neutralised polymer becomes water-soluble, and hence the polymer chain expands due to the mutual repulsion of the negative charges along the backbones. When the HASE polymer is in a solution form, and at a concentration greater than a critical value, the hydrophobic moieties along the polymer backbone associate intermolecularly to form a network structure, which greatly increases the solution viscosity. Because of this unique effect, it has become a very attractive system for many industrial applications.

Being a polyelectrolyte, the HASE system is sensitive to the presence of salt. The concentration of salt in the solution has a profound effect on the network structure and hence on its solution properties. Recently, Tirtaatmadja et al. [8, 28] reported rheological measurements on a HASE polymer and discussed the striking rheological behaviour observed under shear. The dissolution behaviour of a HASE emulsion with a $C_{20}H_{41}$ hydrophobe has recently been studied by Horiuchi et al. [29].

The backbone of the HASE polymer onto which hydrophobic macromonomers are grafted is generally a copolymer of methacrylic acid (MAA) and ethyl acrylate (EA). These polymers exist as insoluble latex particles after synthesis where the pH is usually less than 4. A base can be used to neutralise the MAA groups yielding charged carboxylate groups along the backbone. The solubilisation behaviour of these particles is dependent on the thermodynamic interactions between the monomeric units of the polymers and the solvent (in this case, water) and the electrostatic interactions between charges along the backbone. A series of model polymers consisting of MAA/EA of various molecular weights was synthesized to study the role of molecular weight on the dissolution behaviour of the dispersion in the presence of a base. Conductometric and potentiometric titrations followed by static and dynamic LLS experiments were conducted on this polymer in the presence and absence of salt.

Experimental

Materials

The polymers are designated as RDJ-106, 107, 108 and 111: the details are given in Table 1 and the chemical structure is shown in Fig. 1. The synthesis process of this polymer system is identical to that used in the preparation of model HASE polymers previously reported by Jenkins et al. [30] and Tirtaatmadja et al. [8] The only difference is that in the present synthesis, no hydrophobic macromonomer was used. The molar ratio of MAA:EA is 0.49:0.51. The chain-transfer agent iso-octyl mercapto propionate (IOMP) was added to the MAA/EA monomer mix and fed together with the monomers into the reaction vessel during polymerisation. The amount of IOMP used varied from 0 to 8 wt%. The final emulsions consisted of about 10 wt% solids whose particle size was between 60 and 80 nm for the four batches of polymer produced.

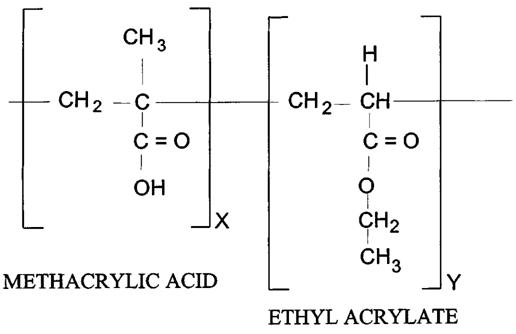

Fig. 1 Chemical structure of a model alkali-soluble emulsion polymer

Table 1 Summary of model methacrylic acid/ethyl acetate copolymers prepared by emulsion polymerisation

Samples	% iso-octyl mercapto propionate	% solids (wt%)	pH	$\langle R_h \rangle$ (nm)	$10^{-4}M_w^a$ (g/mol)
RDJ-106	8.0	9.80	2.3	40.0	0.60
RDJ-108	1.0	9.78	2.3	32.5	4.20
RDJ-111	0.5	9.70	2.2	40.0	11.8
RDJ-107	0.0	9.82	2.2	32.5	30.2

[a] Molecular weight of a single polymer chain determined by static light scattering

The latex emulsion was dialysed against 30 l deionised water for 4 weeks in a cellulose tubular membrane. A series of different polymer concentrations were prepared by dilution of solutions of dialysed RDJ samples with deionised water, using 0.1 mM KCl. The molecular weights of RDJ-107, 111, 108 and 106 were determined by static LLS using a Zimm plot and were found to be 3.02×10^5, 1.18×10^5, 4.20×10^4 and 6.10×10^3 g/mol, respectively. Details of each of the polymer samples are summarised in Table 1. The molecular weight of the polymer decreases with increasing amount of chain-transfer agent.

Instrumentation

Titrations

In the titration of the polymer dispersion, 100 ml 0.1–0.4 g/l test sample was placed in a 250-ml beaker equipped with a magnetic stirrer and was maintained at 25 °C using a refigerated circulating water bath. Titrants consisting of 0.1 ml 0.1 M NaOH were added to the 100-ml test sample via a 5-ml of precision syringe. Potentiometric and conductometric signals were recorded 5 min after each dose had been added using an Orion model 230A pH meter and a Copenhagen CDM 83 conductivity meter. Samples of about 2–3 ml were removed at various stages of the titration for particle size analysis.

Laser light scattering

A commercial light-scattering spectrometer (Brookhaven BI-200M equipped with a BI9000AT multi-τ digital time-correlator) with an argon ion laser operating at 488 nm as the light source was used for this study. The primary beam was vertically polarised with respect to the scattering plane (the optical table surface in this case). For LLS studies, all the polymer samples were centrifuged at 3000 rpm for 4–5 h to remove dust. For static LLS, the instrument was calibrated with toluene to ensure that the scattering intensity from toluene had no angular dependence in the angular range 20–150°. The details of the LLS instrumentation and theory can be found elsewhere [31, 32]. All the measurements were carried out at 25 ± 0.1 °C. In all the LLS experiments, 0.2 g/l (0.02 wt%) latex was used for the determination of the radius of gyration, R_g, and the hydrodynamic radius, R_h. At such dilute concentrations, particle–particle interaction is negligible and hence does not affect the determination of the particle size.

The angular dependence of the excess absolute time-averaged scattered intensity, known as the excess Rayleigh ratio, $R_{vv}(q)$, of a dilute polymer solution can be measured at different concentrations, c (g/ml), and scattering angles θ. $R_{vv}(q)$ is related to the weight-average molecular weight, M_w, by [33]

$$\frac{Kc}{R_{vv}(q)} = \frac{1}{M_w}\left(1+\frac{1}{3}\langle R_g^2\rangle q^2\right) + 2A_2 c \ , \qquad (1)$$

where $K = 4\pi^2 n^2 (\mathrm{d}n/\mathrm{d}c)^2/(N_A \lambda_0^4)$ and $q = (4\pi n/\lambda_0)\sin(\theta/2)$ with N_A, $\mathrm{d}n/\mathrm{d}c$, n and λ_0 being the Avogadro number, the specific refractive index increment, the solvent refractive index and the wavelength of light in vacuo, respectively; A_2 is the second virial coefficient; and $\langle R_g^2\rangle_z^{1/2}$ (or written as $\langle R_g\rangle$) is the root mean square z-average radius of gyration of the polymer chain in solution. At constant concentration Eq. (1) can be rewritten as [34]

$$\left[\frac{Kc}{R_{vv}}\right]_{c\to 0} = \frac{1}{M_w}\left(1+\frac{\langle R_g^2\rangle\, q^2}{3}\right) . \qquad (2)$$

By plotting (Kc/R_{vv}) or $(1/I)^{1/2}$ versus q^2, $\langle R_g\rangle$, can be determined. First the intercept $(1/M_w)$ is obtained from the plot of $(1/I)^{1/2}$ versus q^2 by extrapolating q^2 to zero. The intercept $(1/M_w)$ is then substituted into the computed slope, from which $\langle R_g\rangle$ is calculated. In dynamic LLS, the intensity–intensity time correlation function, $G^{(2)}(t,q)$, in the self-beating mode was measured; this has the following form [31, 32]

$$G^{(2)}(t) = A\left[1+\beta\left|g^{(1)}(t)\right|^2\right] \ , \qquad (3)$$

where q is the scattering vector, β is a parameter depending on the coherence of the detection, t is the delay time, $g^{(1)}(t)$ is a normalised first-order electric field time correlation function and A is the measured base line. For a polydisperse sample, $g^{(1)}(t)$ is related to the line-width distribution $G(\Gamma)$ by

$$c(\tau) = g^{(1)}(t) = \int_0^\infty G(\Gamma)\mathrm{e}^{-\Gamma t}\,\mathrm{d}\Gamma \ , \qquad (4)$$

where Γ is the delay rate. The relaxation time, τ, is inversely proportional to the delay rate, Γ.

A Laplace inversion of $g^{(1)}(t)$ can lead to $G(\Gamma)$. For diffusive relaxation, Γ can be written as,

$$\frac{\Gamma}{q^2} = D \ , \qquad (5)$$

where D is the translational diffusion coefficient and q is the scattering angle.

Results and discussion

The pH and conductometric curves of 0.20 g/l and 0.40 g/l RDJ-106 when titrated with successive 0.1-ml amounts of 0.1 M NaOH are shown in Fig. 2. The dependences of pH and conductance are plotted as a function of the degree of neutralisation, α, defined as [NaOH/COOH]. For the two concentrations, the two conductivity curves exhibit a clear inflection at $\alpha = 1.0$. The overlap of the two potentiometric curves shows that pH does not depend on the concentrations. Our potentiometric and conductometric results are in good agreement with the results of Mouri [35] for the titration of nonassociative alkali-soluble emulsion polymers containing copolymerised carboxylic acids and with those of Horiuchi et al. [29] for associative alkali-soluble polymer. The results of the potentiometric and conductometric titrations suggest that morphological changes take place inside the emulsion particles containing carboxyl groups as the pH changes. To verify this, both static and dynamic LLS measurements were carried out for all four RDJ samples.

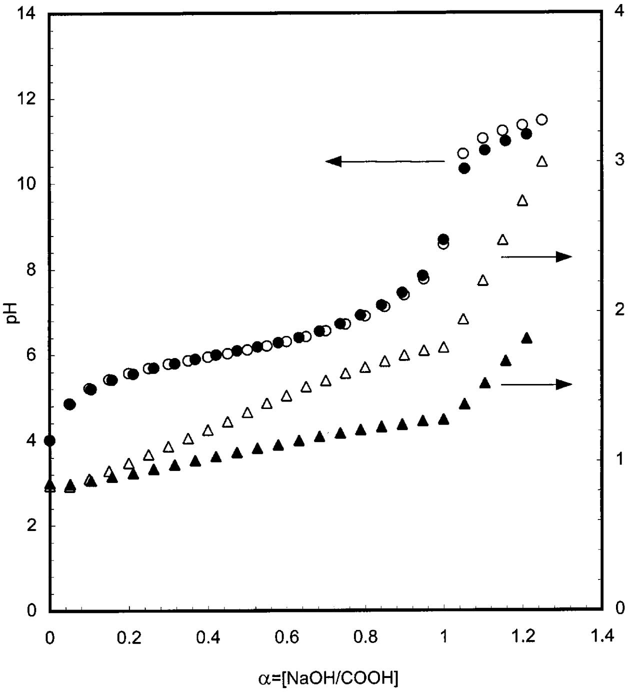

Fig. 2 Potentiometric and conductometric titration of RDJ-106 for c_p = 0.4 g/l (△, ○) and 0.2 g/l (▲, ●) plotted as a function of the degree of neutralisation α = [NaOH/COOH]

$\langle R_g\rangle$ provides information on the evolution of the particle size and the polymer chain conformation. A plot of the inverse of the scattering intensities as a function of scattering angle is shown in Fig. 3. From the slope and the intercept, $\langle R_g\rangle$ could be determined. It should be noted that the measurements were performed from 45 to 120°. The values of qR_g at low degrees of neutralisation (small particles) range from 0.3 to 0.8; however, at high degrees of neutralisation, qR_g ranges from 1.6 to 3.8. Some errors may be expected from the measurements in these ranges. The $\langle R_g\rangle$ values increase with an increase in the degree of neutralisation. This shows that the latex particle swells with the addition of NaOH up to α = 0.4–0.6. Further addition of base beyond this point results in the expulsion of the polymer chains into the bulk solution. The changes in particle size with the addition of NaOH are summarised in Tables 2–5.

A typical plot of the measured intensity–intensity time correlation function for RDJ-107 at $\alpha = 0.5$ in 0.1 mM KCl, at θ = 30° and at a temperature of 25 °C

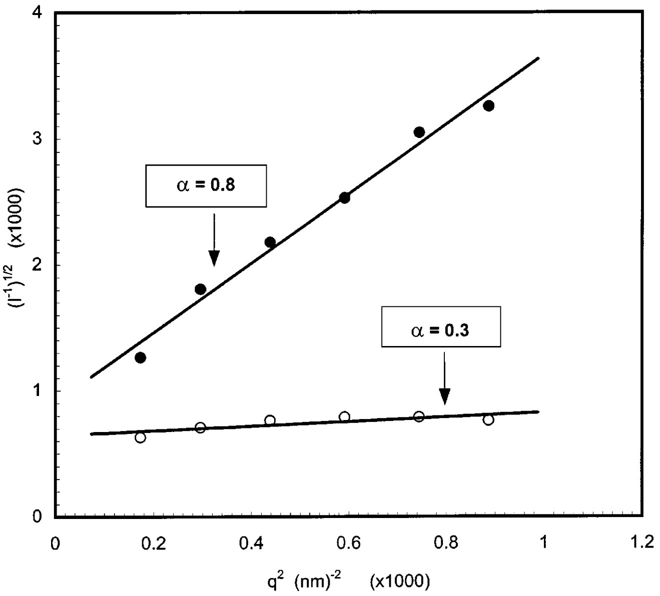

Fig. 3 Typical Berry plots of 0.2 g/l RDJ-111 at α = 0.3 and 0.8 and at 25 °C measured at angles ranging from 45 to 120°

Table 2 Laser light scattering results of RDJ-107 in 0.1 mM KCl at 25 °C

Degree of hydrolysis	$\langle R_g \rangle$ (nm)	$\langle R_h \rangle$ (nm)	$\langle R_g \rangle / \langle R_h \rangle$
0	24.0	32.5	0.74
0.1	26.4	35.0	0.75
0.2	32.6	38.0	0.86
0.3	40.0	60.0	0.67
0.4	55.0	65.0	0.85
0.5	57.5	89.0	0.53
0.6	78.4	108.0	0.73
0.7	87.0	89.0	0.98
0.8	102.0	56.0	1.82
0.9	129.0	55.0	2.35
1.0	92.0	46.0	2.00

Table 3 Laser light scattering results of RDJ-111 in 0.1 mM KCl at 25 °C

Degree of hydrolysis	$\langle R_g \rangle$ (nm)	$\langle R_h \rangle$ (nm)	$\langle R_g \rangle / \langle R_h \rangle$
0	25.0	40	0.63
0.1	26.0	45	0.58
0.2	28.0	56	0.50
0.3	29.0	58	0.50
0.4	31.0	60	0.52
0.5	64.0	57	1.12
0.6	142	89	1.60
0.7	134	89	1.51
0.8	101	50	2.02
0.9	110	47	2.34
1.0	92.0	46	2.00

Table 4 Laser light scattering results of RDJ-108 in 0.1 mM KCl at 25 °C

Degree of hydrolysis	$\langle R_g \rangle$ (nm)	$\langle R_h \rangle$ (nm)	$\langle R_g \rangle / \langle R_h \rangle$
0	20.4	32.5	0.63
0.1	23.6	37.0	0.64
0.2	25.3	40.0	0.63
0.3	27.2	50.0	0.54
0.4	34.0	62.5	0.54
0.5	63.5	62.0	1.02
0.6	102	60.0	1.70
0.7	103	60.0	1.72
0.8	64	35	1.83
0.9	60	30	2.00
1.0	60	30	2.00

Table 5 Laser light scattering results of RDJ-106 in 0.1 mM KCl at 25 °C

Degree of hydrolysis	$\langle R_g \rangle$ (nm)	$\langle R_h \rangle$ (nm)	$\langle R_g \rangle / \langle R_h \rangle$
0	25.0	40.0	0.63
0.1	30.0	41.0	0.73
0.2	38.0	42.0	0.90
0.3	35.0	43.0	0.81
0.4	31.0	57.5	0.54
0.5	31.0	45.0	0.69
0.6	35.0	40.0	0.88
0.7	38.0	30.0	1.27
0.8	41.0	30.0	1.37
0.9	62.0	28.0	2.21
1.0	64.0	28.0	2.29

is shown in Fig. 4a. Using the Laplace inversion program (CONTIN) [36] supplied with the correlator, we calculated the distribution function, $G^{(2)}(t)$, shown in Fig. 4b. Since the delay rate is inversely proportional to the relaxation time, τ, using Eq. (5), $\langle R_h \rangle$ was calculated from the Stokes–Einstein relationship, i.e. $\langle R_h \rangle = k_B T / 6\pi\eta\langle D \rangle$, where k_B, T and η are the Boltzmann constant, the absolute temperature and the solvent viscosity, respectively. The values of $\langle R_h \rangle$ for the four model RDJ polymers are given in Tables 2–5.

Plots of the normalised hydrodynamic radius for the four model RDJ polymers versus degree of neutralisation are shown in Fig. 5. The initial latex hydrodynamic radius is in the range 30–40 nm. As NaOH was added to the emulsion, swelling of the particles occurred over a very short time scale. The swelling is due to the neutralisation of the carboxylic acid groups, which yield negatively charged carboxylate groups. These groups have dual a effects, namely:

1. Inducing solubilisation of the polymer chains by promoting polymer–solvent interactions over the polymer–polymer interactions.

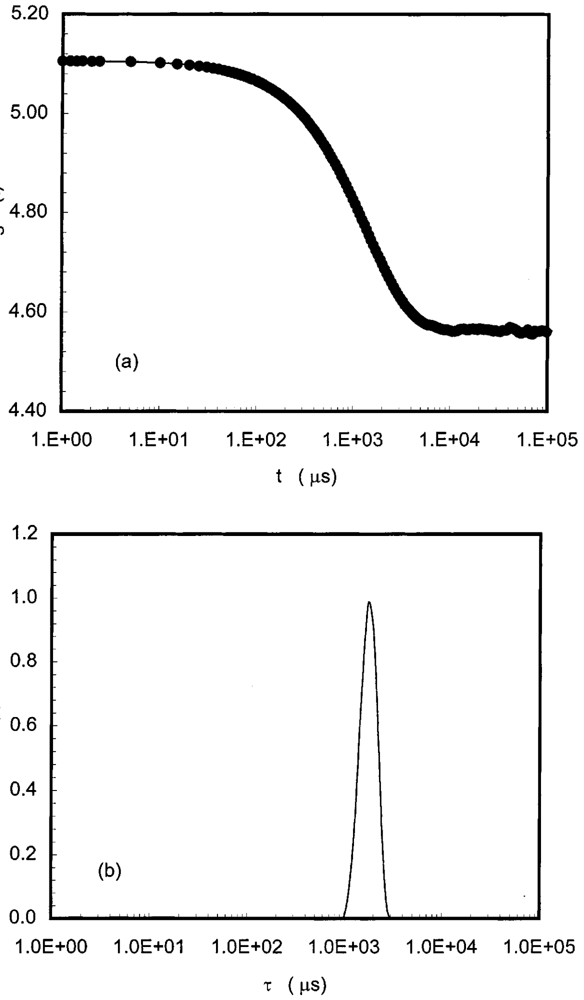

Fig. 4 **a** Typical measured intensity–intensity time correlation function. **b** Laplace inversion using CONTIN analysis of the correlation function for 0.2 g/l RDJ-107 at $\theta = 30°$ and 25 °C

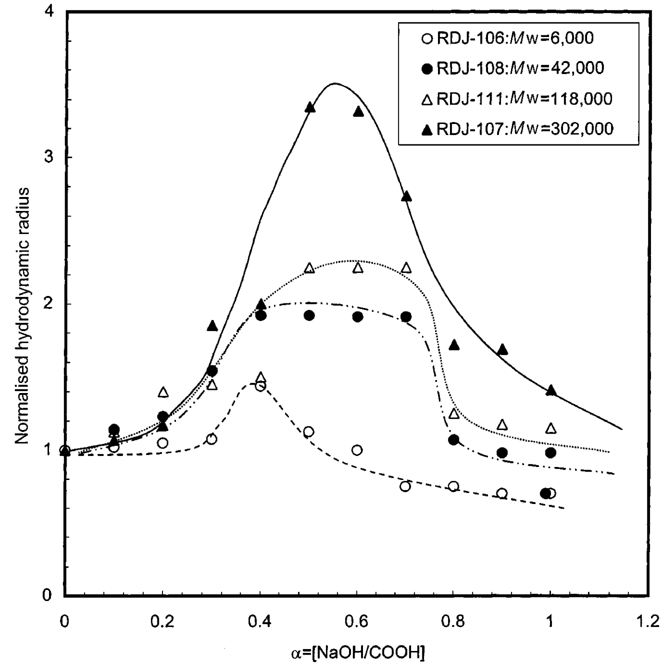

Fig. 5 Plots of hydrodynamic radius, R_h, for four model RDJ polymers versus the degree of neutralisation α = [NaOH/COOH] at 25 °C. Measurements performed on 0.2 g/l samples

2. Enhancing electrostatic repulsion between negatively charged groups along the polymer backbone.

The combination of these two effects causes the particles to swell. The particle size increases and reaches its maximum radius at an α value between 0.4 and 0.6, and the size depends on the molecular weight of the polymer system. Two conclusions could be drawn from the figure:

1. The normalised R_h decreases as the molecular weight decreases. When the molecular weight of individual polymer chains is low, entanglement of these chains in the insoluble particles (consisting of a large number of collapsed polymer chains) is low. The neutralisation of these chains would promote a continuous release of the polymer chains into the bulk solution.
2. The values of α decrease with increasing molecular weight of the polymer. For example, the α value of RDJ-106 (M_w of 6100) is 0.4 while that of RDJ-107 (M_w of 300 200) is 0.6. This seems to indicate that the manner in which the solubilized polymer chains are released into the bulk solution depends on the charge density, which increases with molecular weight.

It is evident that beyond $\alpha = 0.6$, the normalised hydrodynamic radius decreases dramatically; this is associated with the dissolution of the latex into polymer molecules. By combining $\langle R_g \rangle$ from static LLS and $\langle R_h \rangle$ from dynamic LLS, it is apparent that the polymer chain undergoes a transition from a compact to a coiled conformation which eventually becomes an extended polymer chain induced by electrostatic repulsion. At $\alpha = 0$, the ratio $\langle R_g \rangle / \langle R_h \rangle$ is about 0.5–0.7, which suggests that the polymer latex is completely in a collapsed state. With the addition of NaOH, a greater proportion of COOH functional groups are hydrolysed, which gives rise to greater electrostatic repulsion causing the ratio $\langle R_g \rangle / \langle R_h \rangle$ to increase. At $\alpha \cong 0.6$, the value of $\langle R_g \rangle / \langle R_h \rangle$ is in the range 1.2–1.8, indicating that the swollen particle is correlated to that of a coiled conformation [37]. $\langle R_g \rangle / \langle R_h \rangle$ is about 2.0 at $\alpha = 1.0$, indicating that the polymer chains are in an extended coiled chain confirmation due to strong electrostatic repulsion of the negative charges on the polymer backbone. A pictorial representation of the dissolution process for low- and high-molecular-weight polymer systems is summarized in Fig. 6.

Plots of $\langle R_h \rangle$ as a function of the degree of neutralisation for RDJ-107 in 0.001 M (▲), 0.01 M (●) and 0.1 M KCl (■) at 25 °C are shown in Fig. 7. Two observations could be drawn from the figure:

1. $\langle R_h \rangle$ decreases with increasing salt concentrations. This trend suggests that the shielding of the electrostatic repulsion between the COO^- groups by the excess potassium ions reduces the swelling of the particles and also the size of the polymer chains.
2. The degree of neutralisation where the hydrodynamic radius reaches its maximum decreases with increasing salt concentration. For example, the α value for 0.001 M KCl is about 0.55–0.60 compared to 0.3 for 0.1 M KCl. The results suggests that the presence of salt alters the swelling and the expulsion of polymer chains from the swollen particles in the presence of NaOH.

The neutralisation and swelling of the emulsion particles in low- and high-salt environments is summarised in Fig. 8. It is apparent from the present studies that the dissolution of MAA/EA is highly dependent on the size of the polymer chains and the nature of the solvent environment.

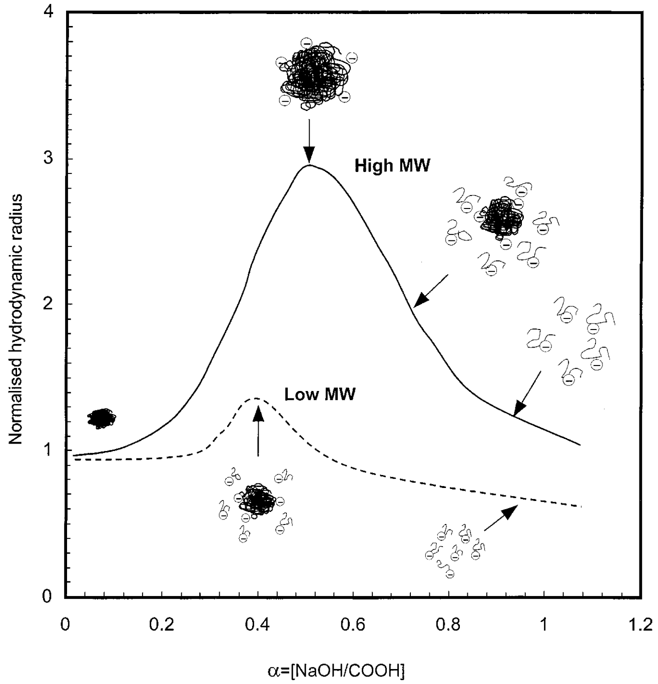

Fig. 6 Schematic representation of the dissolution mechanism of low- and high-molecular-weight (*MW*) methacrylic acid (*MAA*) ethyl acetate (*EA*) polymer systems

Conclusions

The dissolution behaviour of four model alkali-soluble polymer emulsions was studied. The particles sizes were in the range 30–40 nm at $\alpha = 0$, and gradually increased to an optimum size at $\alpha = 0.50$, beyond which the

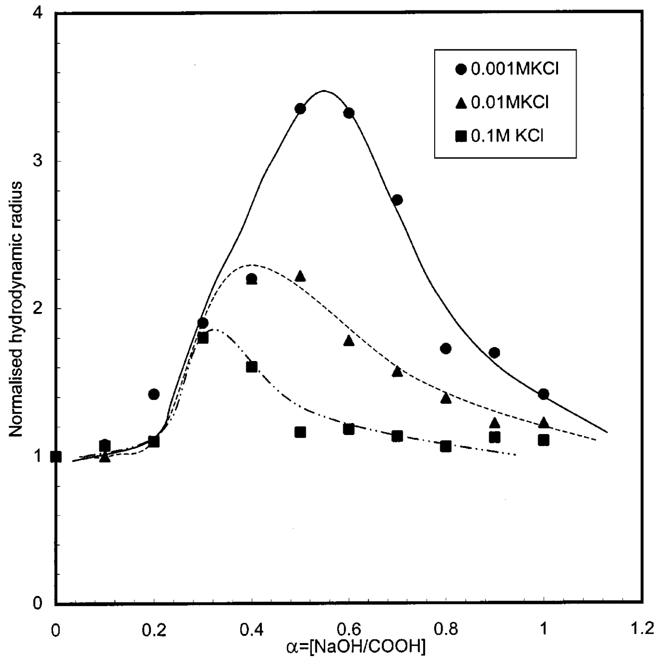

Fig. 7 Plots of $\langle R_h \rangle$ for RDJ-107 at three different salt concentrations and at 25 °C. Measurements performed on 0.2 g/l samples

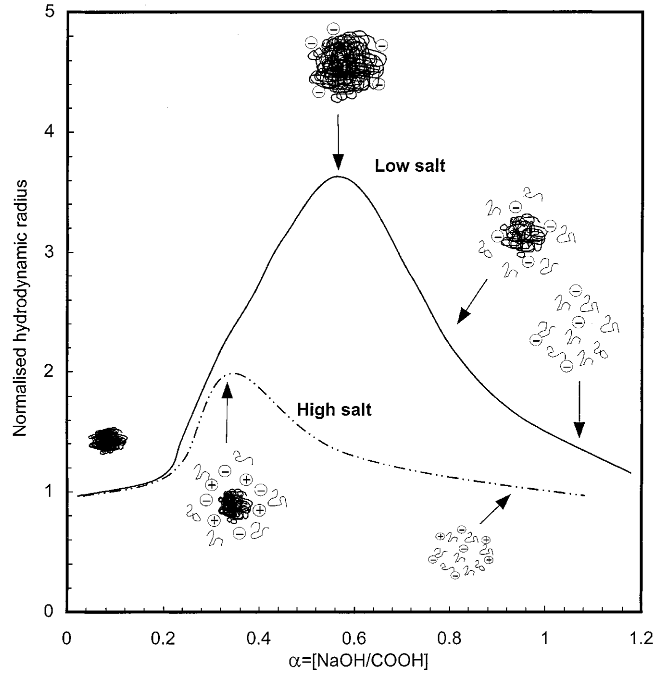

Fig. 8 Schematic representation of the dissolution mechanism of the MAA/EA polymer system in low- and high-salt environments

swollen particles started to disintegrate. By combining the static and dynamic LLS results, we found that the polymer latex is initially in the collapsed state at $\alpha = 0$. It changes to a random coiled chain conformation at $\alpha \sim 0.5$ and finally to an extended coiled chain conformation at $\alpha = 1.0$, where all the COOH groups become completely neutralised. The dissolution of low-molecular-weight polymers is faster than that of high-molecular-weight polymers and $\langle R_h \rangle$ decreases with increasing salt concentration.

Acknowlegements We wish to acknowledge the financial support of the National Science and Technology Board, Singapore, and the Ministry of Trade and Tourism, Ontario, which facilitated the collaboration between NTU and the University of Toronto. Mohammad Siddiq also wishes to acknowledge the Government of Singapore for its financial support. He also wishes to acknowledge Gomal University, Pakistan, for granting him a 1 year sabbatical leave.

References

1. Glass JE (ed) (1986) Water-soluble polymer. Advances in Chemistry 213. American Chemical Society, Washington, D.C.
2. Glass JE (ed) (1989) Polymer in aqueous media. American Chemical Society, Washington, D.C.
3. Glass JE (ed) (1996) Hydrophobic polymer: performance with environmental acceptance. American Chemical Society, Washington, D.C.
4. Schulz DN, Glass JE, (eds) (1991) Polymer as rheology modifier. American Chemical Society, Washington, D.C.
5. Jenkins RD (1991) PhD thesis. Leigh University, Bethlehem, Pa
6. Jenkins RD, Silebi CA, El-Aasser MS (1989) Polym Mater Sci Eng 61:629–633
7. Xu B, Li L, Zhang K, Macdonald PM, Winnik MA, Jenkins RD, Bassett DR, Wolf D, Nuyken O (1997) Langmuir 13:6896–6902
8. Tirtaatmadja V, Tam KC, Jenkins RD (1997) Macromolecules 30:3271–3282
9. Volpert E, Selb J, Candau F (1998) Polymer 39:1025–1033
10. English RJ, Gulati HS, Jenkins RD, Khan SA (1997) J Rheol 41:427–444
11. Vorobyova O, Yekta A, Winnik MA, Lau W (1998) Macromolecules 31:8998–9007
12. Winnik MA, Yekta A (1997) Curr Opin Colloid Interface Sci 2:424–436
13. Tam KC, Jenkins RD, Winnik MA, Bassett DR (1998) Macromolecules 31:4149–4159
14. Jenkins RD, Silebi CA, El-Aasser MS (1990) In: El-Aasser MS (ed) Advances in emulsion polymerization and latex technology: 21st annual short course; 1989, Lehigh University, Bethlehem, Pa, 61, pp 629
15. Walderhang H, Hansen FK, Abrahmsen S, Persson K, Stilbs P (1993) J Phys Chem 271:8336–8432
16. Fonnum G, Bakke J, Hansen FK (1993) Colloid Polym Sci 271:380–389
17. Hulden M (1994) PhD thesis. Abo Akadem University, Finland
18. Lundberg DJ (1990) PhD thesis. North Dakota State University
19. Yekta A, Duhamel J, Brochard P, Adjwidjaja H, Winnik MA (1993) Macromolecules 26:1829–1836
20. Yekta A, Duhamel J, Adjwidjaja H, Winnik MA (1995) Macromolecules 28:952–955
21. Nystrom B, Walderhang H, Hansen FK (1993) J Phys Chem 97:7743–7752
22. Serry AP, Yassini M, Hogen-Esch T, Amis E (1992) Macromolecules 25: 4784–4791
23. Persson K, Abrahmsen S, Stilbs P, Hansen FK, Walderhaug H (1992) Colloid Polym Sci 270:465–469
24. Lundberg DJ, Glass JE, Eley RR (1991) J Rheol 35:1255–1274
25. Richey B, Kirk AB, Eisenhart EK, Fitzwater S, Hook J (1991) J Coating Technol 63:31–40
26. Annable T, Buscall R, Ettelaie R, Whittlestone D (1993) J Rheol 377:695–726
27. Hulden M (1994) Colloids Surf A 82:263–277
28. Tirtaatmadja V, Tam KC, Jenkins RD (1997) Macromolecules 30:1426–1433
29. Horiuchi K, Rharbi R, Yekta A, Winnik MA, Jenkins RD, Bassett DR (1999) Can J Chem 76:1779–1787
30. Jenkins RD, Delong LM, Bassett DR (1996) In: Glass JE (ed) Hydrophilic polymers: performance with Environmental Acceptability. Advances in Chemistry Series 248. American Chemical Society, Washington, D.C., p 425
31. Pecora R, Berne J (1976) Dynamic light scattering. Plenum, New York
32. Chu B (1991) Laser light scattering, 2nd edn. Academic Press, New York
33. Zimm BH (1948) J Chem Phys 16:1099–1104
34. Berry GC (1966) J Chem Phys 11:4550–4561
35. Muori S (1966) J Appl Polym Sci 10:713–729
36. (a) Provencher SW (1976) Biophys J 16:27–32; (b) Provencher SW (1976) J Chem Phys 64:2772–2779
37. Schmidt M, Stockmayer WH (1984) Macromolecules 17:509–514